ARMY RESEARCH LABORATORY

First Principles Calculation of Stress Induced Amorphization in Armor Ceramics

by D. E. Taylor, T. W. Wright, and J. W. McCauley

ARL-MR-0779 **May 2011**

NOTICES

Disclaimers

The findings in this report are not to be construed as an official Department of the Army position unless so designated by other authorized documents.

Citation of manufacturer's or trade names does not constitute an official endorsement or approval of the use thereof.

Destroy this report when it is no longer needed. Do not return it to the originator.

Army Research Laboratory
Aberdeen Proving Ground, MD 21005

ARL-MR-0779 **May 2011**

First Principles Calculation of Stress Induced Amorphization in Armor Ceramics

D. E. Taylor and J. W, McCauley
Weapons and Materials Research Directorate, ARL

T. W. Wright
Adjunct Research Professor, Johns Hopkins University

REPORT DOCUMENTATION PAGE	*Form Approved OMB No. 0704-0188*

1. REPORT DATE *(DD-MM-YYYY)*	2. REPORT TYPE	3. DATES COVERED (From - To)
May 2011	DRI	FY10

4. TITLE AND SUBTITLE	5a. CONTRACT NUMBER
First Principles Calculation of Stress Induced Amorphization in Armor Ceramics	5b. GRANT NUMBER
	5c. PROGRAM ELEMENT NUMBER

6. AUTHOR(S)	5d. PROJECT NUMBER
D. E. Taylor, T. W. Wright, and J. W. McCauley	5e. TASK NUMBER
	5f. WORK UNIT NUMBER

7. PERFORMING ORGANIZATION NAME(S) AND ADDRESS(ES)	8. PERFORMING ORGANIZATION REPORT NUMBER
U.S. Army Research Laboratory ATTN: RDRL-WML-B Aberdeen Proving Ground, MD 21005	ARL-MR-0779

9. SPONSORING/MONITORING AGENCY NAME(S) AND ADDRESS(ES)	10. SPONSOR/MONITOR'S ACRONYM(S)
	11. SPONSOR/MONITOR'S REPORT NUMBER(S)

12. DISTRIBUTION/AVAILABILITY STATEMENT

Approved for public release; distribution unlimited.

13. SUPPLEMENTARY NOTES

14. ABSTRACT

Recent experimental work within the U.S. Army Research Laboratory has identified the formation of nanoscale-sized intragranular amorphous bands leading to a marked reduction in ballistic performance of boron carbide (B_4C). This pressure-induced amorphization has been examined through application of the Born stability criterion that imposes restrictions on the relative magnitudes of the elastic constants of a stable crystal. The analysis has been conducted for B_4C as a function of structural polytype using ab initio solid-state density functional methods and the results of the pressure evolution of the B_4C elastic constants are reported. It is shown that the C-C-C polytype, a minority phase in the B_4C lattice, fails at a pressure of ≈20 gigapascals less than the other polytypes tested in this survey, indicating that it may serve as one of the initial points of failure upon impact.

15. SUBJECT TERMS

Boron carbide, amorphization, elastic constant

16. SECURITY CLASSIFICATION OF:			17. LIMITATION OF ABSTRACT	18. NUMBER OF PAGES	19a. NAME OF RESPONSIBLE PERSON
a. REPORT	b. ABSTRACT	c. THIS PAGE			D. E. Taylor
Unclassified	Unclassified	Unclassified	UU	24	19b. TELEPHONE NUMBER (*Include area code*) (410) 306-0853

Contents

List of Figures

List of Tables

Acknowledgments

All calculations were run at the Engineer Research and Development Center (ERDC) Defense Shared Resource Center using computer time granted by the High Performance Computing and Modernization Program.

INTENTIONALLY LEFT BLANK.

1. Objective

Boron carbide (BC), due to its extreme hardness and low density, has been used as an armor ceramic for many years. Its elastic properties, which surpass more dense compounds such as silicon carbide by a factor of 2, suggest that BC should sustain high impact pressures without failure; however, there is an anomalous loss of impact resistance within the material, apparently due to increased fragmentation by a factor of 2 to 3. Recent experimental work within the U.S. Army Research Laboratory has identified the formation of nanoscale-sized intragranular amorphous bands as the primary damage mechanism leading to the marked reduction in ballistic performance of BC (*1*, *2*). The Army has a need to understand the mechanism for the formation of these amorphous bands, *at the atomic level*, which will allow for the design of chemically modified BC materials that will show improved impact resistance and, hence, improved armor ceramic performance. Using first principles quantum mechanics, we provide much needed insight into the formation mechanism of the experimentally observed amorphous bands that are known to weaken BC ceramics. In particular, the stress-induced amorphization of BC is explored via application of the "Born instability" criterion, which requires that the matrix of second derivatives of the energy per unit cell be positive definite, where the six independent variables are strain measures in the current configuration. A material that exhibits a Born instability loses its ability (at some stress and temperature) to convert certain incremental strain patterns into stress increments. These strain patterns are known as "soft" modes of deformation, which must be related to movements within the atomic structure. Identification of the onset and nature of the Born instability will give further insight into the formation mechanism of the amorphous regions that weaken the BC material. In this research, we examine the influence of both pressure and shear stress on the Born instability.

2. Approach

BC, with nominal stoichiometry B_4C, consists of 12-atom icosahedra crosslinked by 3-atom chains (figure 1) and belongs to the crystallographic space group R-3m (*3*). The exact nature of the 3-atom chain is unknown experimentally due to the close spectroscopic signatures of boron and carbon. The crystal structure consists of a mixture of B_{12} icosahedra linked by C-C-C chains and $B_{11}C$ icosahedra linked with C-B-C chains (among others). For the C-B-C "polytype," there is an additional complication; the location of the carbon atom in the $B_{11}C$ cage is not known. This, again, is due to the difficulty in definitively resolving boron and carbon; therefore, the carbon atom inserted into the cage could reside in one of two symmetry unique centers, the so-called *polar* and *equatorial* sites within the icosahedron, as shown in figure 1. It should be noted that although BC is generally regarded to have R-3m symmetry, this is only true for the C-C-C

polytype and placement of a carbon atom within the icosahedra causes a distortion of the rhombohedral lattice and the actual structure is dictated by an averaging of all the different polytypes.

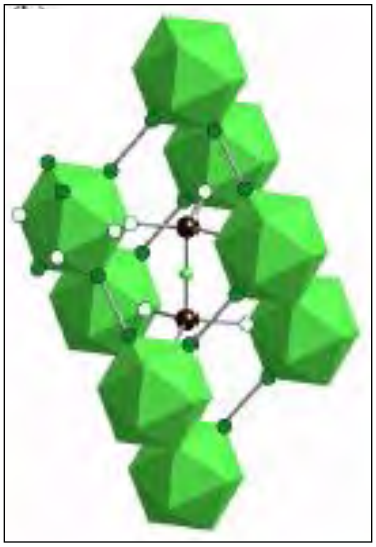

Figure 1. Icosahedral structure of BC. Polar and equatorial sites in the icosahedra are indicated by dark green and white spheres, respectively.

As a route to the elucidation of the mechanism by which pressure and shear induce an amorphous transition in BC, we have applied the Born-stability criterion to each of the three polytypes discussed earlier. Born showed that an expansion of the internal energy of a crystal in a power series in the strain, along with the imposition of positivity of the energy, leads to restrictions on the relative magnitudes of the elastic constants of a stable crystal (*4*). The existence of such a Born instability can be determined quantum mechanically.

BC is highly anisotropic elastically and for crystals with R-3m symmetry, there are only six non-zero independent elastic constants $\{\mathbf{C}_{ij}\}$ for the unloaded material (*5*). These constants have been determined experimentally for BC, except for the modulus c_{14} (*6*). Each of the elastic moduli varies independently with pressure, and at some point, the system may reach a structural instability. Imposition of the Born stability conditions leads to the following restrictions on the elastic constants for a stable crystal with R-3m symmetry:

$$C_{11} - |C_{12}| > 0 \tag{1}$$

$$(C_{11} + C_{12})C_{33} - 2C_{13}*C_{13} > 0 \tag{2}$$

$$(C_{11} - C_{12})C_{44} - 2C_{14}*C_{14} > 0 \tag{3}$$

The procedure previously adopted by others is to compute the six elastic constants above as a function of pressure and evaluate equations 1 through 3 to determine the onset of the instability, i.e., the pressure at which one or more of the equations above are no longer valid (*7, 8*). Once

the initial instability has been located, evaluation of the ―soft modes" of deformation (atomic displacements corresponding to the instability) can be determined.

Equations 1–3 are generally not applicable to the incremental moduli of crystals under finite loading; however, a general indicator of an elastic instability for all materials under any state of loading is

$$\det | \mathbf{C} | = 0, \tag{4}$$

where **C** is the full 6x6 tensor of incremental elastic moduli (*9, 10*). Further, since the determinant of a matrix is equal to the product of its eigenvalues, an equivalent statement of equation 4 is that all the eigenvalues of **C** must be positive and the first stress state at which an eigenvalue equals zero corresponds to an instability. It should be noted that for a crystal under load, the elastic constant tensor **C** should be replaced by the ―effective" elastic constant tensor **B** given by

$$B_{ijkl} = C_{ijkl} + (1/2)(\delta_{ik}\tau_{jl} + \delta_{jk}\tau_{il} + \delta_{il}\tau_{jk} + \delta_{jl}\tau_{ik} - 2\delta_{kl}\tau_{ij}) \tag{5}$$

with τ_{ij} being an element of the stress tensor (*10*).

The elastic constants were computed using the CP2K software package (*11*). Density functional theory using the Perdew-Burke-Ernzerhof (PBE) functional (*12*) in a double zeta valence plus polarization basis set was used for all calculations with a planewave cutoff of 800 Rydberg. Elastic constants are related to the second derivative of the total energy with respect to strain, ε_i, via

$$C_{ij} = \frac{1}{V}\frac{\partial^2 E}{\partial \varepsilon_i \partial \varepsilon_j}\bigg|_0 , \tag{6}$$

where V is the unit cell volume and i,j=1…6 in the Voigt notation (*13*). The CP2K software does not evaluate elastic constants analytically; therefore, a Fortran program was written for this work that evaluates the second derivative of the energy with respect to strain (equation 6) via a finite difference of analytic first derivatives provided by the CP2K code. This new program includes the required stress corrections from equation 5 in the computation of the elastic constants, computes the bulk modulus using the Voigt-Reuss-Hill approximation (*14*), and finally determines the eigenspectrum of the elastic tensor. Since we have used the finite difference approach, the *full* 6x6 elastic constant tensor can be evaluated with only 6 quantum mechanical (QM) calculations (12 if double-sided differences are taken, as is done in this work). This is much less than the *minimum* 43 calculations required using a strain energy approach advocated by some authors.

3. Results

The optimized lattice parameters for each polytype are presented in table 1. The theoretical structures computed using PBE are in excellent agreement with experiment (*3*) and the distortion of the lattice from purely rhombohedral symmetry is clearly evident in the polar and equatorial polytypes. Lazzari et al. conducted a computational study and concluded that the polar polytype is the most stable configuration energetically (*15*). This is also supported by our results where it is found that the C-C-C and equatorial polytypes lie 71 and 35 meV/atom higher in energy than the polar configuration, respectively.

Table 1. Unit cell parameters of BC polytypes (lengths in angstrom, angles in degrees volume in cubic angstroms).

Polytype	a	b	c	alpha	beta	gamma	Volume
CCC	5.196	5.196	5.196	66.00	66.00	66.00	112.12
Polar	5.070	5.215	5.215	65.24	66.07	66.07	109.75
Equatorial	5.176	5.213	5.213	64.87	64.96	64.96	110.17
Experiment	5.19	5.19	5.19	65.18	65.18	65.18	110.02

Each polytype was subjected to hydrostatic compression and the resulting pressure-volume data was fitted to the third order Birch-Murnaghan equation of state (*16*). As shown in figure 2, the pressure response of each polytype is very similar. The computed bulk moduli for each polytype (and its associated pressure derivative resulting from the Birch-Murnaghan fit) are presented in table 2 and compare exceptionally well with the experimental value. The polar and equatorial polytypes, both with C-B-C chains, have bulk moduli that are marginally different; however, the C-C-C polytype has a reduction of ≈12 GPa, indicating that it is softer than the other polytypes. It has been suggested that the C-C-C polytype, a minority phase in the BC crystal, is the ~~"~~weakest link" in the structure and may be the polytype that fails first when impacted. The lower bulk modulus is in support of that hypothesis however more rigorous evidence will be provided in the following.

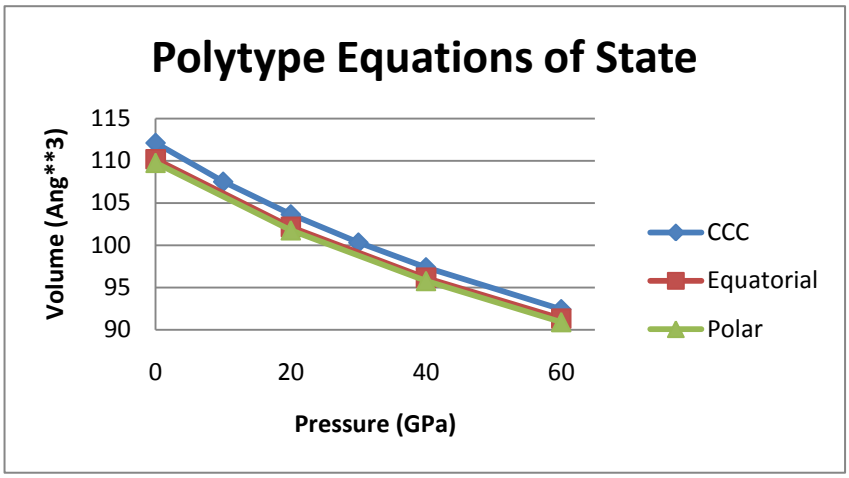

Figure 2. Equations of state for each polytype.

Table 2. Bulk modulus and pressure derivative resulting from Birch-Murnaghan equation of state fit to DFT data.

Polytype	Bulk Modulus (GPa)	Pressure Derivative
CCC	222	3.5
Polar	234	3.3
Equatorial	233	3.4
Experiment	236	

The elastic moduli of BC have been evaluated experimentally by McClellan et al. (*6*); however, in their analysis, they assumed a hexagonal symmetry (due to limitations in their fitting software), which leaves the value of the C_{14} elastic constant indeterminate (*5*). Since elastic constants are tensor quantities that depend on orientation, *in order to have a direct comparison with experiment,* we have used a hexagonal setting of the rhombohedral BC unit cell in the initial QM calculations. This does not change any of the conclusions resulting from the stability analysis since the eigenvalues are invariant to any orthogonal transformation of the coordinate axes; it simply allows us to use the experimental values as a metric by which the accuracy of our computed elastic constants can be measured. (We have computed values for C_{14} using the proper rhombohedral setting, however.) The theoretical and experimental elastic constants are presented in table 3. The agreement with experimental values is excellent; however, it should be noted that our theoretical values are for idealized structures with perfect B_4C stoichiometry, whereas the experimental values were obtained from single crystalline measurements of a sample with stoichiometry $B_{5.6}C$ (*6*). This will invariably affect the experimental results as compared to a perfect B_4C stoichiometry, though it is not clear to what extent.

The pressure evolution of the elastic constants over the 0–80 GPa range for each polytype is shown in figure 3. There we show, for the first time, that for the BC ceramic each C_{ij} increases with pressure however the C_{44} and C_{66} moduli show a marked decrease. This pressure softening of elastic moduli (C_{44} in particular) has been observed experimentally (as well as theoretically) in alpha quartz which is known to undergo pressure induced amorphization similar to the phenomenon observed in BC.

Table 3. Theoretical and experimental elastic constants (GPa).
(The non-zero C_{14} modulus is indeterminate in this orientation.)

Cij	**CCC**	**Polar**	**Equatorial**	**Exp.**
C11	487	554	559	543
C12	117	121	117	131
C13	66	65	70	64
C33	525	526	521	535
C44	133	155	153	165
C66	183	216	218	206

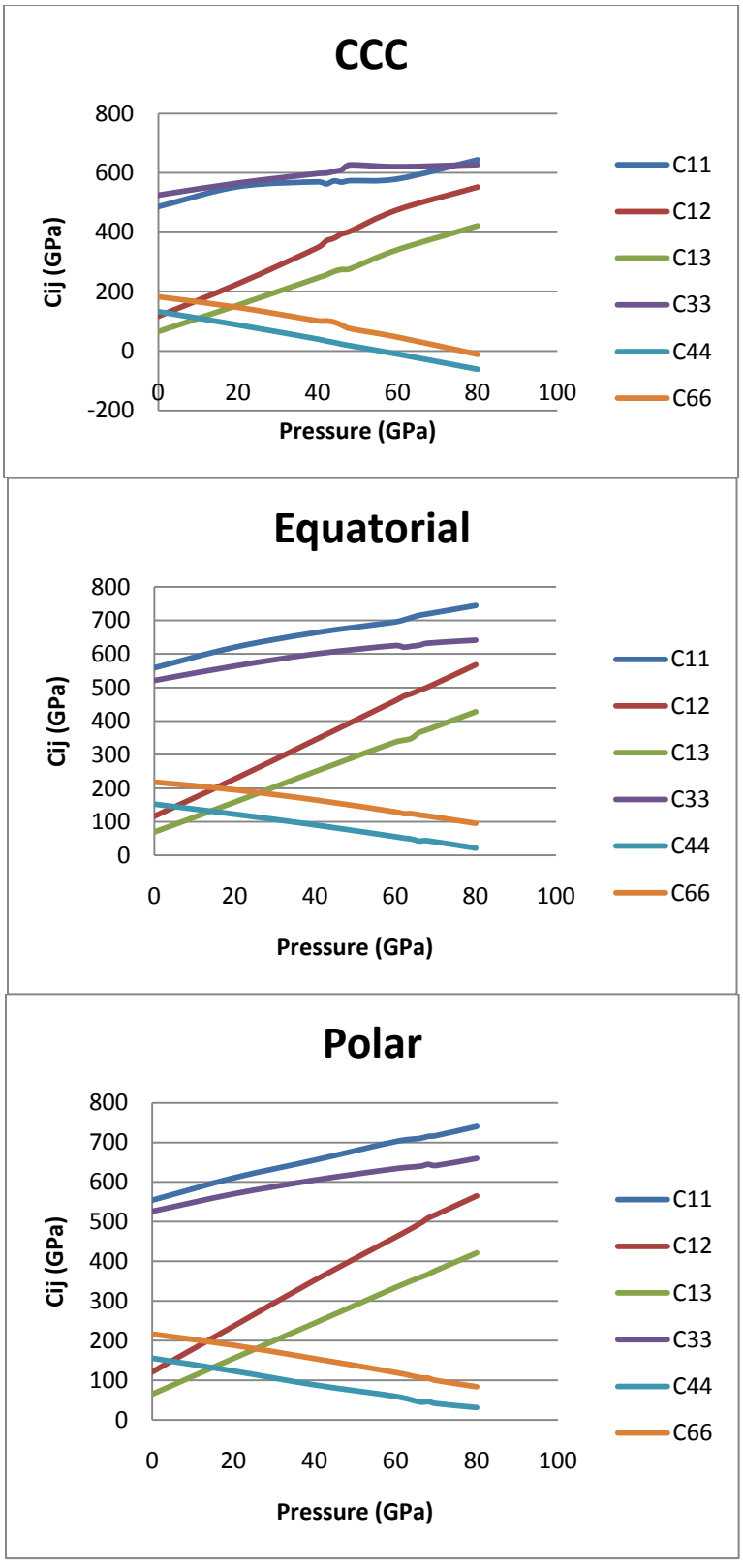

Figure 3. Pressure evolution of the elastic moduli for each polytype.

The lowest eigenvalue of the elastic constant tensor for each polytype is plotted as a function of pressure in figure 4. For each polytype the eigenvalue decreases monotonically towards zero and reaches zero between 44–46 GPa for the C-C-C polytype and between 66–68 and 68–70 GPa for the equatorial and polar polytypes, respectively, indicating that the C-C-C polytype reaches an elastic instability at much lower pressures than the other polytypes and is the initial point of failure in the BC ceramic under hydrostatic loading. This is in support of the work of Fanchini et al., who studied the stability of BC polytypes relative to the segregated boron and carbon phases (*17*). In their work they demonstrated that the C-C-C polytype is relatively unstable energetically as compared to the polar and equatorial configurations as a function of hydrostatic load.

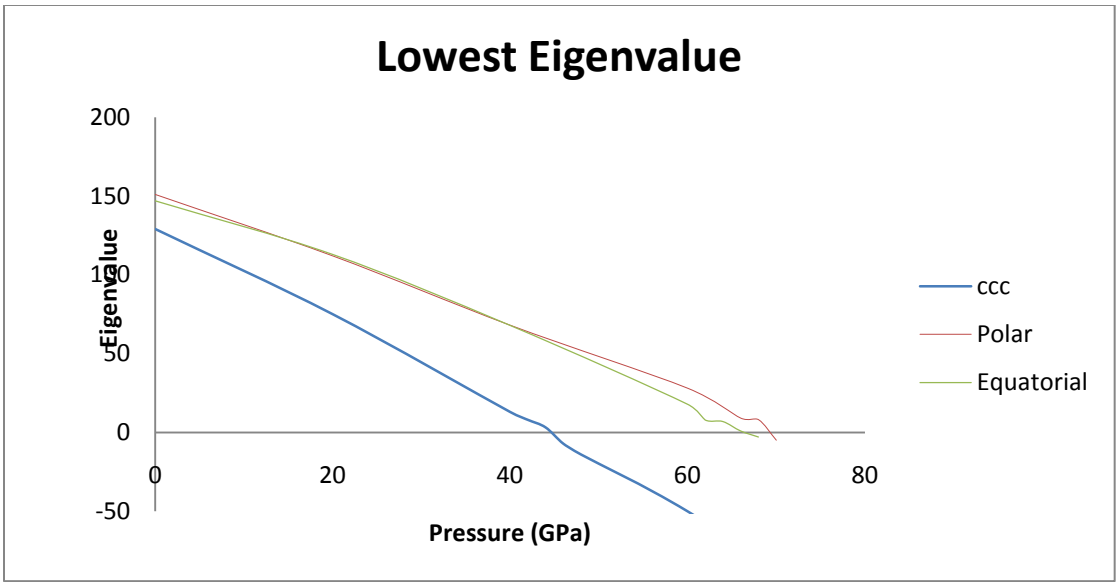

Figure 4. Lowest eigenvalue of elastic constant tensor for each polytype.

4. Conclusions

Our calculations thus far have outlined the mechanical response of BC under hydrostatic compression as a function of polytype; however, it has been suggested that shear plays a critical role in weakening the BC ceramic. Our preliminary results lend support to this hypothesis. Specifically, examination of the eigenvectors associated with the soft mode eigenvalues plotted in figure 4 show a significant contribution from shear and indicates that loading along these shearing modes may hasten amorphization. Future work will attempt to construct an amorphization contour in a selected two-dimensional (2-D) pressure—shear space. It now appears feasible to use theoretical constitutive representations from nonlinear elasticity to minimize the QM calculations so that full exploration of the six-dimensional (6-D) stress space is unnecessary.

The stability analysis conducted herein allows for identification of the stress at which amorphization may initiate; however, one of our ultimate goals is to relate changes in the local atomic structure to the root cause of the instability. For example, Binggeli et al. (*7*) studied the pressure-induced amorphization phenomenon in α-quartz and presented evidence that a shear instability was the driving force toward collapse of the material. Specifically, when subjected to shear, silicon atoms were displaced towards oxygen atoms, leading to a change in silicon coordination. Previous theoretical work on BC showed that under uniaxial loading the icosahedra remain relatively unaltered; however, there *was* a bending of the 3-atom chain that eventually led to the formation of new covalent bonds between the chain atoms and boron atoms in the icosahedra (*18*). This type of structural rearrangement can lead to an irreversible alteration of the lattice, which may trigger the collapse of BC leading to amorphization. This rearrangement mechanism needs further study and molecular dynamics simulation, where the change in structural morphology can be studied in real time, is an ideal method for this analysis. However, this is entirely contingent upon the availability of an accurate interatomic potential applicable to BC.

This work has shown that the C-C-C polytype is in fact the weakest polytype within the BC structure; however, these results are based on idealized structures with perfect B_4C stoichiometry. In the actual material, there is a high degree of substitutional disorder as well as defect sites consisting of vacancies in the atomic chain linking the icosahedra. A computational survey of the possible defect polytypes within BC has been conducted by Saal et al. (*19*); however, their worked focused on structure, enthalpy of formation, and phonon spectra. Therefore, calculations of the mechanical properties of these additional structures are required for a complete stability analysis of the BC ceramic.

5. References

1. Moynihan, T. J.; LaSalvia, J. C.; Burkins, M. S. Analysis of Shatter Gap Phenomenon in a B_4C/Composite Laminate Armor System. *20th ISB*, Orlando, FL. 23–27 Sept. 2002.
2. Chen, M.; McCauley, J. W.; Hemker, K. J. Shock-induced Localized Amorphization in Boron Carbide. *Science* **2003**, *299*, 1563.
3. Clark, H. K.; Hoard, J. L. The Crystal Structure of Boron Carbide. *J. Am. Cer. Soc* **1943**, *65*, 2115.
4. Born, M.; Huang, K. *Dynamical Theory of Crystal Lattices*; Oxford University Press: London, 1954.
5. Nye, J. F. *Physical Properties of Crystals*; Oxford at the Clarendon Press, (1957).
6. McClellan, K. J.; Chu, F.; Roper, J. M.; Shindo I. Room Temperature Single Crystal Elastic Constants of Boron Carbide. *J. Mat. Sci.* **2001**, *36*, 3403.
7. Binggeli, N.; Chelikowsky, J. R. Elastic Instability in α-Quartz Under Pressure. *Phys. Rev. Lett.* **1992**, *69*, 2220.
8. Tse, J. S.; Klug, D. D. Mechanical Instability of α-Quartz: A Molecular Dynamics Study. *ibid* **1991**, *67*, 3559.
9. Wang, J.; Li, J.; Yip, S. Mechanical Instabilities of Homogenous Crystals. *Phys. Rev. B* **1995**, *52*, 12627.
10. Wang, J.; Yip, S.; Phillpot, S. R.; Wolf, D. Crystal Instabilities at Finite Strain. *Phys. Rev. Lett.* **1993**, *71*, 4182.
11. CP2K is freely available from http://cp2k.berlios.de/ (accessed January, 2010).
12. Perdew, J. P.; Burke, K.; Ernzerhof, M. Generalized Gradient Approximation Made Simple. *Phys. Rev. Lett.* **1996**, *77*, 3865.
13. Perger, W. F.; Criswell, J.; Civalleri, B.; Dovesi, R. Ab Initio Calculation of Elastic Constants of Crystalline Systems with the CRYSTAL Code. *Comp. Phys. Comm.* **2009**, *180*, 1753.
14. Hill, R. The Elastic Behaviour of a Crystalline Aggregate. *Proc. of the Phys. Soc. A* **1952**, *65*, 349.
15. Lazzari, R.; Vast, N.; Besson, J. M.; Baroni, S.; Dal Carso, A. Atomic Structure and Vibrational Properties of Icosahedral B_4C Boron Carbide. *Phys. Rev. Lett.* **1999**, *83*, 3230.

16. Birch, F. Finite Elastic Strain of Cubic Crystals. *Phys. Rev.* **1947**, *71*, 809.

17. Fanchini, G.; McCauley, J. W.; Chhowalla, M. Behavior of Disordered Boron Carbide Under Stress. *Phys. Rev. Lett.* **2006**, *97*, 035502.

18. Yan, X. Q.; Tang, Z.; Zhang, L.; Guo, J. J.; Jin, C. Q.; Zhang, Y.; Goto, T.; McCauley, J. W.; Chen, M. W. Depressurization Amorphization of Single-Crystal Boron Carbide. *ibid* **2009**, *102*, 075505.

19. Saal, J. E.; Shang, S.; Liu, Z. The Structural Evolution of Boron Carbide Via Ab Initio Calculations. *App. Phys. Lett.* **2007**, *91*, 231915.

6. Transitions

Results of this work will be presented at the 35th International Conference and Exposition on Advanced Ceramics and Composites (Taylor, 2011) and at the American Society of Mechanical Engineers (ASME) Applied Mechanics and Materials Conference (Wright, 2011).

NO. OF COPIES ORGANIZATION

1 (PDF only) DEFENSE TECHNICAL INFORMATION CTR
DTIC OCA
8725 JOHN J KINGMAN RD
STE 0944
FORT BELVOIR VA 22060-6218

3 US ARMY RSRCH LAB
ATTN IMNE ALC HRR
MAIL & RECORDS MGMT
ATTN RDRL CIM L TECHL LIB
ATTN RDRL CIM P TECHL PUB
ADELPHI MD 20783-1197

1 ODUSD (SANDT) WS
L SLOTER
ROSSLYN PLAZA N
STE 9030
1777 N KENT ST
ARLINGTON VA 22209-2210

1 COMMANDER
US ARMY MATERIEL CMD
AMXMI INT
9301 CHAPEK RD
FT BELVOIR VA 22060-5527

1 PEO GCS
SFAE GCS BCT/MS 325
M RYZYI
6501 ELEVEN MILE RD
WARREN MI 48397-5000

1 ABRAMS TESTING
SFAE GCSS W AB QT
J MORAN
6501 ELEVEN MILE RD
WARREN MI 48397-5000

1 COMMANDER
WATERVLIET ARSENAL
SMCWV QAE Q
B VANINA
BLDG 44
WATERVLIET NY 12189-4050

2 COMMANDER
US ARMY AMCOM
AVIATION APPLIED TECH DIR
J SCHUCK
FT EUSTIS VA 23604-5577

NO. OF COPIES ORGANIZATION

1 NAVAL SURFACE WARFARE CTR
DAHLGREN DIV CODE G06
DAHLGREN VA 22448

1 USA SBCCOM PM SOLDIER SPT
AMSSB PM RSS A
J CONNORS
KANSAS ST
NATICK MA 01760-5057

2 UNIV OF DELAWARE
DEPT OF MECH ENGR
J GILLESPIE
NEWARK DE 19716

3 AIR FORCE ARMAMENT LAB
AFATL DLJW
W COOK
D BELK
J FOSTER
EGLIN AFB FL 32542

1 DPTY ASSIST SCY FOR R&T
SARD TT
ASA (ACT)
J PARMENTOLA
THE PENTAGON RM 3E479
WASHINGTON DC 20310-0103

1 US ARMY ARDEC
AMSTA AR AE WW
E BAKER
BLDG 3022
PICATINNY ARSENAL NJ
07806-5000

11 US ARMY TARDEC
AMSTRA TR R MS 263
K BISHNOI
D TEMPLETON (10 CPS)
WARREN MI 48397-5000

1 COMMANDER
US ARMY RSRCH OFC
A RAJENDRAN
PO BOX 12211
RSRCH TRIANGLE PARK NC
27709-2211

NO. OF
COPIES ORGANIZATION

2 CALTECH
G RAVICHANDRAN
T AHRENS MS 252 21
1201 E CALIFORNIA BLVD
PASADENA CA 91125

5 SOUTHWEST RSRCH INST
C ANDERSON
K DANNEMANN
T HOLMQUIST
G JOHNSON
J WALKER
PO DRAWER 28510
SAN ANTONIO TX 78284

3 SRI INTERNATIONAL
D CURRAN
D SHOCKEY
R KLOOP
333 RAVENSWOOD AVE
MENLO PARK CA 94025

1 APPLIED RSRCH ASSOCIATES
D GRADY
4300 SAN MATEO BLVD NE
STE A220
ALBUQUERQUE NM 87110

1 INTERNATIONAL RSRCH
ASSOCIATES INC
D ORPHAL
4450 BLACK AVE
PLEASANTON CA 94566

1 BOB SKAGGS CONSULTANT
S R SKAGGS
7 CAMINO DE LOS GARDUNOS
SANTA FE NM 87501

2 WASHINGTON ST UNIV
INST OF SHOCK PHYSICS
Y GUPTA
J ASAY
PULLMAN WA 99164-2814

1 COORS CERAMIC CO
T RILEY
600 NINTH ST
GOLDEN CO 80401

NO. OF
COPIES ORGANIZATION

1 UNIV OF DAYTON
RSRCH INST
N BRAR
300 COLLEGE PARK
MS SPC 1911
DAYTON OH 45469-0168

2 COMMANDER
US ARMY TACOM
AMSTA TR S
T FURMANIAK
L PROKURAT FRANKS
WARREN MI 48397-5000

1 PROJECT MANAGER
ABRAMS TANK SYSTEM
J ROWE
WARREN MI 48397-5000

3 COMMANDER
US ARMY RSRCH OFC
B LAMATINA
D STEPP
W MULLINS
PO BOX 12211
RSRCH TRIANGLE PARK NC
27709-2211

1 NAVAL SURFACE WARFARE CTR
CARDEROCK DIVISION
R PETERSON
CODE 28
9500 MACARTHUR BLVD
WEST BETHESDA MD 20817-5700

4 LAWRENCE LIVERMORE NATL LAB
R GOGOLEWSKI L290
R LANDINGHAM L369
J E REAUGH L282
S DETERESA
PO BOX 808
LIVERMORE CA 94550

4 SANDIA NATL LAB
J ASAY MS 0548
L CHHABILDAS MS 0821
D CRAWFORD ORG 0821
M KIPP MS 0820
PO BOX 5800
ALBUQUERQUE NM 87185-0820

NO. OF
COPIES ORGANIZATION

3 RUTGERS
THE STATE UNIV OF NEW JERSEY
DEPT OF CRMCS & MATLS ENGRNG
R HABER
607 TAYLOR RD
PISCATAWAY NJ 08854

2 THE UNIVERSITY OF TEXAS
AT AUSTIN
S BLESS
IAT
3925 W BRAKER LN STE 400
AUSTIN TX 78759-5316

3 SOUTHWEST RSRCH INST
C ANDERSON
J RIEGEL
J WALKER
6220 CULEBRA RD
SAN ANTONIO TX 78238

1 CERCOM
R PALICKA
991 PARK CENTER DR
VISTA CA 92083

6 GDLS
W BURKE MZ436 21 24
G CAMPBELL MZ436 30 44
D DEBUSSCHER MZ436 20 29
J ERIDON MZ436 21 24
W HERMAN MZ435 01 24
S PENTESCU MZ436 21 24
38500 MOUND RD
STERLING HTS MI 48310-3200

1 INTERNATL RSRCH ASSN
D ORPHAL
4450 BLACK AVE
PLEASANTON CA 94566

1 JET PROPULSION LAB
IMPACT PHYSICS GROUP
M ADAMS
4800 OAK GROVE DR
PASADENA CA 91109-8099

3 OGARA HESS & EISENHARDT
G ALLEN
D MALONE
T RUSSELL
9113 LE SAINT DR
FAIRFIELD OH 45014

NO. OF
COPIES ORGANIZATION

2 CERADYNE INC
M NORMANDIA
3169 REDHILL AVE
COSTA MESA CA 96626

3 JOHNS HOPKINS UNIV
DEPT OF MECH ENGRNG
K T RAMESH
T W Wright
3400 CHARLES ST
BALTIMORE MD 21218

2 SIMULA INC
V HORVATICH
V KELSEY
10016 51ST ST
PHOENIX AZ 85044

3 UNITED DEFENSE LP
E BRADY
R JENKINS
K STRITTMATTER
PO BOX 15512
YORK PA 17405-1512

10 NATL INST OF STANDARDS & TECH
CRMCS DIV
G QUINN
STOP 852
GAITHERSBURG MD 20899

2 DIR USARL
AMSRD ARL D
C CHABALOWSKI
V WEISS
2800 POWDER MILL RD
ADELPHI MD 20783-1197

NO. OF
COPIES ORGANIZATION

ABERDEEN PROVING GROUND

65 DIR USARL
RDRL WM
S KARNA
J MCCAULEY (10 CPS)
J SMITH
RDRL WMB
J NEWILL
M ZOLTOSKI
D TAYLOR (10 CPS)
RDRL WMM
S MCKNIGHT
R DOWDING
RDRL WMM C
R SQUILLACIOTI
RDRL WMM D
E CHIN
K CHO
G GAZONAS
J LASALVIA
P PATEL
J MONTGOMERY
J SANDS
RDRL WMS
T JONES
RDRL WMT
P BAKER
B BURNS
RDRL WMT A
P BARTKOWSKI
M BURKINS
W GOOCH
D HACKBARTH
T HAVEL
C HOPPEL
E HORWATH
M KEELE
D KLEPONIS
H MEYER
J RUNYEON
S SCHOENFELD
RDRL WMT C
T BJERKE
T FARRAND
K KIMSEY
L MAGNESS
S SEGLETES
D SCHEFFLER
R SUMMERS
W WALTERS
RDRL WMT D
J CLAYTON
D DANDEKAR
M GREENFIELD
E RAPACKI
M SCHEIDLER
T WEERASOORIYA
RDRL SL
R COATES